APPLIED PHYSICS LETTERS VOLUME 83, NUMBER 16 20 OCTOBER 2003

Electron spin resonance observation of trapped electron centers in atomic-layer-deposited hafnium oxide on Si

A. Y. Kang[a)] and P. M. Lenahan
The Pennsylvania State University, University Park, Pennsylvania 16802

J. F. Conley, Jr.
Sharp Labs of America, Camas, Washington 98607

(Received 2 June 2003; accepted 27 August 2003)

We observed two paramagnetic defects in thin films of HfO_2 on silicon with electron spin resonance. Both appear after photoinjecting electrons into the dielectric. Strong spectroscopic evidence links one spectrum to an O_2^- defect. A second spectrum is likely due to an Hf^{+3} related defect. © *2003 American Institute of Physics.* [DOI: 10.1063/1.1621078]

The scaling down of device dimensions which has enabled the microelectronic industry to follow Moore's Law for over thirty years cannot continue much longer. The International Technology Roadmap for Semiconductors indicates that a fundamental physical limit to the downscaling of conventional SiO_2-based gate dielectric thickness will be reached by 2005.[1] A solution to this problem may be the utilization of high dielectric constant materials which would allow physically thicker films to be used as the gate dielectric.[1] Several candidate materials show the greatest promise: Al_2O_3, ZrO_2, and HfO_2. Among these dielectrics, HfO_2 is favored because it has a higher dielectric constant ($\sim$20) than Al_2O_3 ($\sim$9), and is more stable against silicide formation than ZrO_2.[2,3] HfO_2 also exhibits lower leakage currents than SiO_2 at an equivalent oxide thickness.[4]

Previous work by our group and several others indicates high densities ($\geqslant 10^{12}/cm^2$) of electron traps in HfO_2/Si films.[4–8] These electron traps are an important reliability issue and possibly a fundamental physical limit for high-*k* dielectric-based transistors. Our results[5] on atomic-layer-deposited (ALD) films indicate electron trap densities ($>2\times10^{12}\ cm^{-2}$) and that trapped electrons stay trapped over long periods of time. Electron trapping was also reported in samples quite similar to those utilized in this study by Conley *et al.*[4] in HfO_2 film subject to constant voltage stress. Another recent study by Zafar *et al.*[6] reported positive threshold voltage shifts in *n*-field effect transistor devices, also in ALD HfO_2 gate dielectrics, resulting from high electric field stressing. They argue that the trapping of charges occurs at existing traps, and that their experimental procedure did not create additional traps. Zhu *et al.*[7] recently reported positive flat-band voltage shifts which they attribute to negative effective-trapped charge in jet vapor deposited HfO_2 films; they reported a trapped electron density saturating at $\sim 2\times10^{12}\ cm^{-2}$ for all samples in their study. Earlier, Gusev *et al.*[8] reported high electron trap densities in HfO_2-based transistors. They report that, at low stress voltages, electrons fill existing traps, with the creation of traps being observed at higher stress voltages.

The physical and chemical nature of the electron traps in HfO_2/Si systems remains largely a mystery. We have initiated an investigation of charge trapping in ALD HfO_2/Si using electron spin resonance (ESR)[9] and capacitance–voltage ($C-V$) measurements. In this work, we report trap densities and capture cross section of electron trap(s), as well as ESR data identifying defects which likely play a major role in the electron trapping in the HfO_2/Si system.

High resistivity (111) 3 in. substrates and much lower resistivity, 4–30 Ω cm (100) p-Si 6 in. substrates were utilized for ESR and electrical measurements, respectively. For all measurements, bare HfO_2 films were deposited via ALD using $Hf(NO_3)_4$ as a precursor at a substrate temperature of approximately 170 °C. The samples received a 420 °C post-deposition N_2 anneal for 60 s, and the thickness was determined by spectroscopic ellipsometry. Electrical samples were 25.6 nm±0.6 nm; ESR samples were 42.7 nm±0.1 nm. More information about deposition and film characterization can be found elsewhere.[4,10] We utilized the ultraviolet light/corona ion technique to inject charge into the dielectric films.[11] ESR measurements are facilitated by the use of bare oxides, and the ultraviolet light/corona ion technique eliminates the requirement of a metal gate electrode. A mercury probe was used to form a temporary gate electrode to make $C-V$ measurements at 100 kHz. ESR measurements were made at the X band at 150 Kelvin.

$C-V$ flat-band voltages versus electron fluence are illustrated in Fig. 1. With the simplifying assumptions that trap density is uniform throughout the dielectric and that only a single trap capture cross section need be considered, the flat-band voltage shift may be described by

$$\Delta V_{FB}=\left[\frac{N_t e}{C_{ox}2}\right](1-e^{-\sigma\eta}), \tag{1}$$

where C_{ox} is the oxide capacitance per unit area, N_t is the number of traps per unit area, e is electronic charge, σ is the capture cross-section, and η is the fluence (charge carriers injected per unit area). The solid line in Fig. 1 is a plot of the ΔV_{FB} versus fluence as obtained by Eq. (1). Figure 1 indicates that ΔV_{FB} versus fluence can be fit to a curve corre-

---

[a)] Electronic mail: ayk101@psu.edu

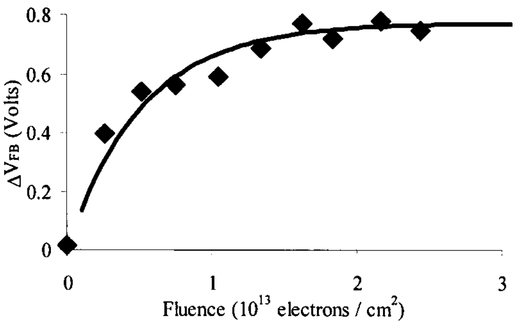

FIG. 1. Flat-band voltage shift vs electron fluence for a 25.6 nm ALD HfO_2 film. The ΔV_{FB} data can be fit to a curve obtained [from Eq. (1)] (solid line) with capture cross section σ of 3×10^{-13} cm^2 and trap density N_t of 2×10^{12} cm^{-2}.

sponding to a capture cross section σ of 3×10^{-13} cm^2 and trap density of $N_t=2\times10^{12}$ cm^{-2}, implying simply filling of pre-existing traps.

Figure 2 illustrates ESR spectra generated by the electron injection. The same electron injection procedure was used for the ESR measurements and for the $C-V$ measurements of Fig. 1. However, as mentioned previously, ESR samples were somewhat thicker and were grown on high resistivity substrates to enhance the sensitivity of the measurement. The fairly complex pattern presented in Fig. 2 corresponds to two different center spectra. ESR spectra are, in part, characterized by g tensors. The g tensor for the signal on the left-hand side in Fig. 2(a) is $g_{zz}=2.04$, $g_{yy}=2.01$, and $g_{xx}=2.000$. The g tensor is defined by

$$g=h\nu/\beta H, \tag{2}$$

where h is Planck's constant, ν is the microwave frequency, β is the Bohr magneton, and H is the magnetic field at which resonance is observed. The g value varies with the orientation of the defect geometry and applied magnetic field; the relationship can be described by a second rank tensor. A computer simulation of a spectrum expected for a randomly oriented array of defects with this g tensor is illustrated in Fig. 2(b). The simulation was carried out using WINEPR SimFonia simulation software of Bruker Instruments (Billercia, MA).

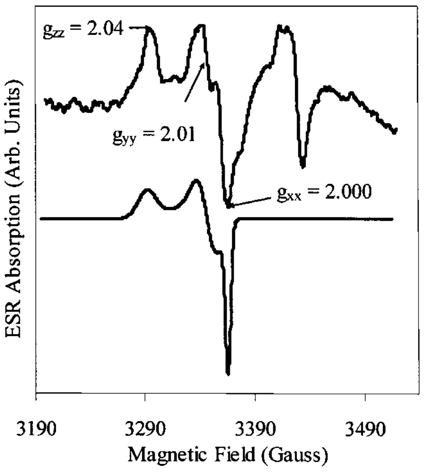

FIG. 2. (a) ESR trace generated by electron photoinjection at an electron fluence of 2×10^{13} cm^{-2}. (b) Simulated ESR spectra with $g_{zz}=2.04$, $g_{yy}=2.01$, and $g_{zz}=2.000$.

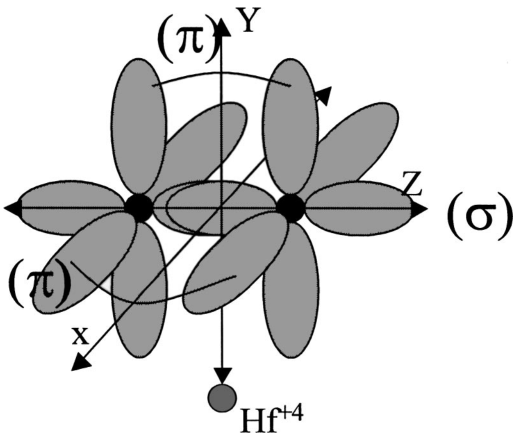

FIG. 3. Schematic diagram of the π wave functions for an O_2^- molecule defect.

Numerous ESR studies of O_2^- centers in materials with ionic bond characteristics have identified ESR spectra similar to ours, as due to O_2^- ions coupled to cations.[12–23] Kanzig and Cohen[24] have derived expressions for the g tensor for O_2^- ion defects, based on the electronic ground-state energy levels for the O_2^- in an ionic system as depicted by Fig. 3. The Kanzig and Cohen model should hold for HfO_2, since the Hf—O bond has 70% ionic character. As Fig. 3 illustrates, the O_2^- ion has both σ and π bonding. The crystal field around the defect removes the degeneracy of the π bonding and antibonding levels, splitting the $2p\pi_g$ orbitals by an energy Δ, as shown in Fig. 4. Following the energy level diagram of Fig. 4, Kanzig and Cohen derived the expressions for the g tensors:[24]

$$g_{xx}=g_e\left(\frac{\Delta^2}{\lambda^2+\Delta^2}\right)^{1/2}-\frac{\lambda}{E}\left[-\left(\frac{\lambda^2}{\lambda^2+\Delta^2}\right)^{1/2}-\frac{\Delta}{(\lambda^2+\Delta^2)^{1/2}}+1\right], \tag{3}$$

$$g_{yy}=g_e\left(\frac{\Delta^2}{\lambda^2+\Delta^2}\right)^{1/2}-\frac{\lambda}{E}\left[\left(\frac{\lambda^2}{\lambda^2+\Delta^2}\right)^{1/2}-\frac{\Delta}{(\lambda^2+\Delta^2)^{1/2}}-1\right], \tag{4}$$

$$g_{zz}=g_e+2\left(\frac{\lambda^2}{\lambda^2+\Delta^2}\right)^{1/2}\ell, \tag{5}$$

where $g_e=2.0023$ is the free electron g value, λ is the spin–orbit coupling of oxygen (usually taken to be 0.014). The

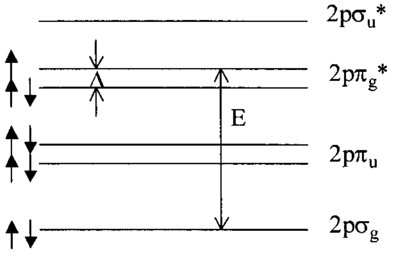

FIG. 4. Electronic energy levels of the O_2^- defect.

energy level separations E and Δ are defined in Fig. 4. The parameter ℓ is a correction to the angular momentum about z caused by the crystal field and is normally close to one.[22–24] In general, $\lambda<\Delta\ll E$, and thus to a first-order approximation, Eqs. (3)–(5) may be simplified to yield: $g_{\mathrm{xx}}\cong g_e$, $g_{\mathrm{yy}}\cong g_{\mathrm{e}}+2\lambda/E$, and $g_{\mathrm{zz}}\cong g_{\mathrm{e}}+2\lambda/\Delta$.

Thus, g_{xx} is usually very close to the free electron $g=2.0023$, and g_{yy} is generally shifted somewhat higher than the free electron; its value is typically about 2.01 ± 0.001. As indicated by the simplified Eq. (5), the magnitude of the g_{zz} component is greatly influenced by the local surroundings which results in the crystal-field splitting Δ, and is thus a good indicator of the environment surrounding the O_2^- ion. The larger the electronic crystal field present at the defect site, the smaller the deviation of g_{zz} from the free electron value.

The Kanzig and Cohen model for the O_2^- ion has been widely accepted in literature dealing with these centers in many ionic materials.[12–24] ESR characterization of the O_2^- ion in ionic materials has been reviewed by Lunsford[22] and Che and Tench.[23] Of particular interest to our work, ESR measurements of the O_2^- ion in the chemically very similar ZrO_2 system have been reported by several other groups.[18–21] The g tensor, which we assign to O_2^- in HfO_2, $g_{zz}=2.04$, $g_{yy}=2.01$, and $g_{xx}=2.000$, is quite similar to that reported in ZrO_2:[18–21] $g_{zz}\cong2.033$, $g_{yy}\cong2.01$, and $g_{xx}\cong2.003$. As Zr and Hf are chemically similar, the close similarity between the two tensors provides further strong evidence that the HfO_2 ESR spectra is due to an O_2^- defect.

The signal in the far right-hand side of Fig. 2, at a zero crossing $g=1.96$, is also quite similar to a signal previously reported in ZrO_2 systems. A signal with a g tensor of $g_{\parallel}=1.978$ and $g_{\perp}=1.953$ (Refs. 18–21, 25) and a zero crossing of $g=1.953$ has been attributed to a Zr^{+3}-related defect in ZrO_2. The close chemical similarity between Hf and Zr would indicate that Hf^{+3} and Zr^{+3} would have somewhat similar spectra; however, the larger spin–orbit coupling constant of Hf would require a fortuitous scaling of crystal fields to yield such similar g tensors. Therefore, we very tentatively attribute this signal to an Hf^{+3}-related ion defect. This signal, like the Hf/O_2^-, also consistently appears with the electron injection, although the magnitude of the signal does not track with that of the O_2^- ion signal.

The density of O_2^- centers generated by the photoinjection is about $3\times10^{12}/\mathrm{cm}^2$; the density of defects tentatively associated with Hf^{+3} defects is about 10% of that value. Our measurement of spin density is good to about a factor of 2 in absolute number. Since this number is about equal to the number of trapped electrons, presumably $(42.7\ \mathrm{nm}/25.6\ \mathrm{nm})\times2\times10^{12}/\mathrm{cm}^2\approx3\times10^{12}$, our results strongly suggest that O_2^-, clearly a negatively charged defect, is the end result of electron trapping in the HfO_2 dielectric. The appearance of the more tentatively identified Hf^{+3}-related center suggests that it may play a significant role in the electron trapping.

Work at Penn State was sponsored by the Intel Corp. through Semiconductor Research Corporation Custom Funding.

[1] The International Technology Roadmap for Semiconductors, http://public.itrs.org
[2] M. Gutowski, J. E. Jaffe, C.-L. Liu, M. Stoker, R. I. Hegde, R. S. Rai, and P. J. Tobin, Appl. Phys. Lett. **80**, 1897 (2002).
[3] Y.-S. Lin, R. Puthenkovilakam, and J. P. Chang, Appl. Phys. Lett. **81**, 2041 (2002).
[4] J. F. Conley, Jr., Y. Ono, R. Solanki, G. Stecker, and W. Zhuang, Appl. Phys. Lett. **82**, 3508 (2003).
[5] A. Y. Kang, P. M. Lenahan, and J. F. Conley, Jr., IEEE Trans. Nucl. Sci. **49**, 2636 (2002).
[6] S. Zafar, A. Callegari, E. Gusev, and M. V. Fischetti, Tech. Dig. - Int. Electron Devices Meet. **2002**, 517 (2002).
[7] W. J. Zhu and T. P. Ma, IEEE Electron Device Lett. **23**, 597 (2002).
[8] E. P. Gusev, D. A. Buchanan, E. Cartier, A. Kumar, D. DiMaria, S. Guha, A. Callegari, S. Zafar, P. C. Jamison, D. A. Neumayer, M. Copel, M. A. Gribelyuk, H. Okorn-Schmidt, C. D'Emic, R. J. Fleming, A. Mocuta, and A. Ajmera, Tech. Dig. - Int. Electron Devices Meet. **2001**, 451 (2001).
[9] P. M. Lenahan and J. F. Conley, Jr., J. Vac. Sci. Technol. B **16**, 2134 (1998).
[10] J. F. Conley, Jr., Y. Ono, D. J. Tweet, W. Zhuang, and R. Solanki, J. Appl. Phys. **93**, 712 (2003).
[11] R. E. Mikawa and P. M. Lenahan, J. Appl. Phys. **59**, 2054 (1986).
[12] M. Shiotani, G. Moro, and J. H. Freed, J. Chem. Phys. **74**, 2616 (1981).
[13] P. H. Kasai, J. Chem. Phys. **43**, 3322 (1965).
[14] X. Zhang and K. J. Klabunde, Inorg. Chem. **31**, 1706 (1992).
[15] R. F. Howe and M. Gratzel, J. Phys. Chem. **91**, 3906 (1987).
[16] R. F. Howe and W. C. Timmer, J. Phys. Chem. **85**, 6129 (1986).
[17] E. Abi-Aad, R. Bechara, J. Grimblot, and A. Aboukais, Chem. Mater. **5**, 793 (1993).
[18] J. Matta, J. F. Lamonier, E. Abi-Aad, E. A. Zhilinskaya, and A. Aboukais, Phys. Chem. Chem. Phys. **1**, 4975 (1999).
[19] V. Ramaswamy, B. Tripathi, D. Srinivas, A. V. Ramaswamy, R. Cattaneo, and R. Prins, J. Catal. **200**, 250 (2001).
[20] E. Giamello, M. Volante, B. Fubini, F. Geobaldo, and C. Morterra, Mater. Chem. Phys. **29**, 379 (1991).
[21] M. Anpo, M. Che, B. Fubini, E. Garrone, E. Giamello, and M. C. Paganini, Top. Catal. **8**, 189 (1999).
[22] J. H. Lunsford, Catal. Rev.-Sci. Eng. **8**, 135 (1973).
[23] M. Che and A. J. Tench, Adv. Catal. **32**, 1 (1983).
[24] W. Kanzig and M. H. Cohen, Phys. Rev. Lett. **3**, 509 (1959).
[25] C. Morterra, E. Giamello, L. Orio, and M. Volante, J. Phys. Chem. **94**, 3111 (1990).